Measurement of Applied Force and Deflection in the Javelin Throw

Maeda, Masato
Shamoto, Eiji
Moriwaki, Toshimichi
Nomura, Haruo

(Citation)
Journal of Applied Biomechanics,15(4):429-442

(Issue Date)
1999-11

(Resource Type)
journal article

(Version)
Version of Record

JOURNAL OF APPLIED BIOMECHANICS, 1999, 15, 429-442

Measurement of Applied Force and Deflection in the Javelin Throw

Masato Maeda, Eiji Shamoto, Toshimichi Moriwaki, and Haruo Nomura

The present paper presents a new sensor to measure 6 components of force and 2 components of deflection applied to the javelin during the throw. Since the javelin is deflected and vibrated during throwing, measurement of force and deflection applied to the javelin will provide important information for throwers in how to better throw the javelin and to design javelins with better dynamic characteristics. The sensor is designed not to significantly change the static and dynamic characteristics of the javelin. The force sensor performs well in terms of linearity and crosstalk, and the javelin equipped with this sensor has similar characteristics to ordinary javelins. The present paper also presents an example of measurement in the javelin throw.

Key Words: measurement of force, javelin throw, force sensor, deflection of javelin

Hubbard and Bergman (1989) found that the javelin is accelerated and thrown with vibratory deflections. Since the acceleration and the vibrations are products of characteristics of the javelin and the forces applied to the javelin by throwers, it is essential to clarify the characteristics of the javelin (Maeda, Nomura, Moriwaki, and Shamoto, 1993) and to analyze the forces applied to the javelin. The revision of specifications for javelins in 1986 exemplifies this importance. The best performance in 1985 was 96.96 m; after the specification revisions were initiated in 1986, the best performance was reduced to 85.74 m.

While the static (Maeda, Nomura, & Miyagaki, 1990; Terauds, 1985) and dynamic (Maeda et al., 1993) characteristics of the javelin have been studied, inputs to the javelin (i.e., forces) have not been measured. This is mainly because ordinary force sensors are too large and heavy to be attached to the javelin without changing its characteristics. However, the measurement of the forces is crucial in creating accurate simulations of the physical outputs of the javelin such as acceleration, deflected vibrations, and rotation. This measurement and the consequent simulations are expected to give important information about developing better ways to design and throw javelins.

M. Maeda and H. Nomura are with the Faculty of Human Development at Kobe University, Kobe, Japan, 657-8501. E. Shamoto and T. Moriwaki are with the Faculty of Engineering at Kobe University.

A new sensor is designed and developed in the present research to measure six components of force and two components of deflection applied to the javelin in the javelin throw in such a way that the javelin equipped with the sensor has similar characteristics to ordinary javelins, both statically and dynamically.

Development of the New Force Sensor

The measurement of force applied to the javelin by throwers will be useful not only in determining the best throwing motion but also to determine the best characteristics of the javelin for each thrower. However, such measurements are difficult to obtain for the following reasons: (a) Characteristics of the javelin equipped with the force sensor, such as mass, stiffness, moment of inertia, position of center of gravity, and natural frequency, must be close to those of ordinary javelins; (b) the force sensor is deformed due to deflection of the javelin during throwing of the javelin; and (c) the javelin is accelerated in the throwing direction during throwing and vibrated in the normal directions.

Figure 1 shows the force sensor developed in the present research, where the deflection is defined as *Dy* and *Dz* in the *y* and *z* directions, respectively. The middle part of the pipe is gripped by the throwers, and both ends of the pipe are fixed on to the javelin with small bolts so that the gripped part of the pipe does not touch the body of the javelin. The strain gauges are attached to the semicircular beams on both sides of the pipe, and the strain of the beams caused by the force and the deflection applied to the javelin is measured. The present force sensor is designed in order to cope in the following ways with the above mentioned difficulties.

Regarding the first difficulty, the diameter of the javelin around the gripped part is reduced from 30 mm to 26 mm, and the sensor (Figure 1) is installed (Figure 2). As the shape of the beam is kept similar and the dimensions are decreased, the stiffness and the sensitivity are increased, but the load capacity is decreased. Therefore, the thickness/width of the beam is reduced to 3 mm. The width of the strain gauges are 2.4 mm, and the diameter of the semicircular beams is selected to be 10 mm, based on the beam analysis, so that the sensor can bear predicted maximum loads of 1000 N in the *x* direction and 500 N in the *y* and *z* directions.

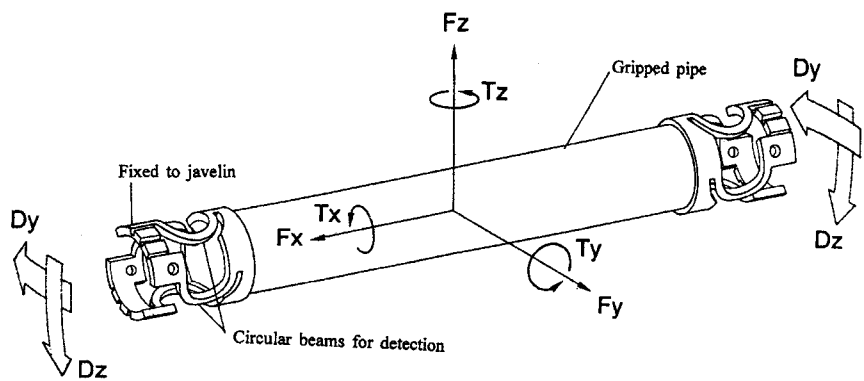

Figure 1 — Overview of developed sensor: Three components of force, three components of torque, and two components of deflection can be measured simultaneously with strain gauges attached to circular beams.

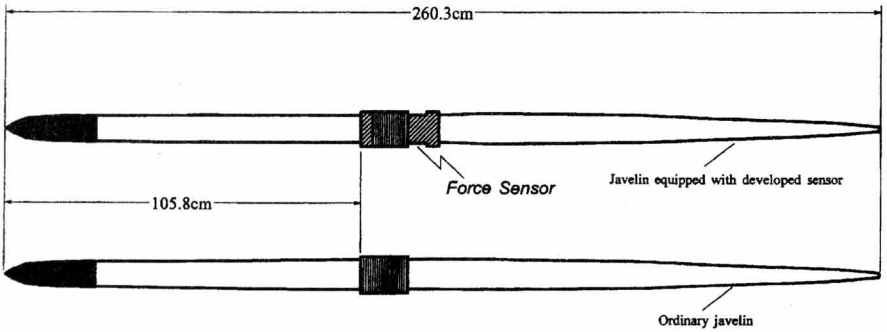

Figure 2 — Javelin equipped with developed sensor and ordinary javelin.

Regarding the second difficulty, the eight semicircular beams shown in Figures 1 and 3 are deformed by not only the six components of the force applied to the grip but also the deflection of the javelin. An example of such superposition is shown in Figure 4. Although all six components of the force and the two components of the deflection are generally superposed during throwing, the eight components cause eight different modes of beam deformation. Thus, the Wheatstone bridge circuits shown in Figure 5 can eliminate crosstalk among the eight components. Figure 6 shows this measuring principle by taking an example of the axial force *Fx*. When *Fx* is applied, all beams are deformed and all the strain gauges have compressive or tensile strain. However, the changes in resistance of the strain gauges are added to each other only in the circuit ϵFx,

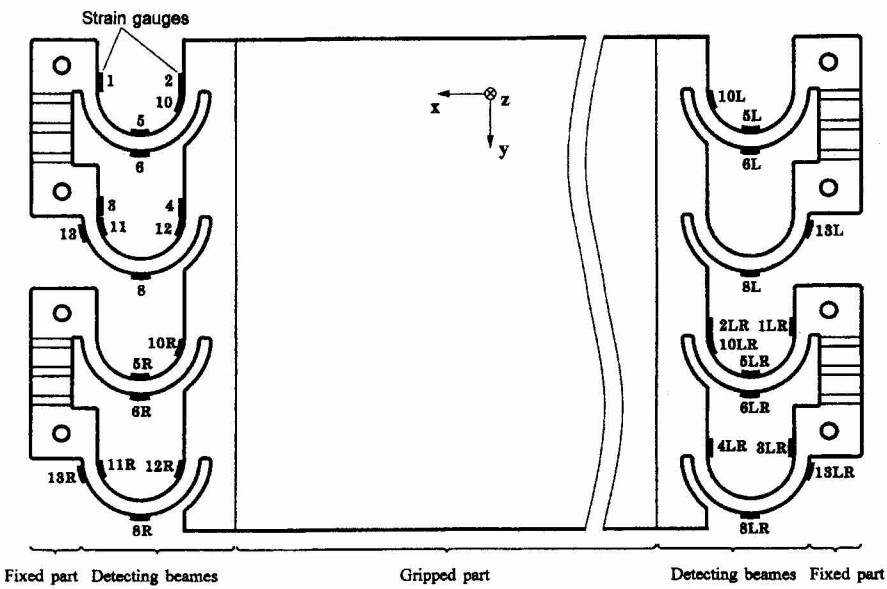

Figure 3 — Development view of force sensor and strain gauges attached to circular beams.

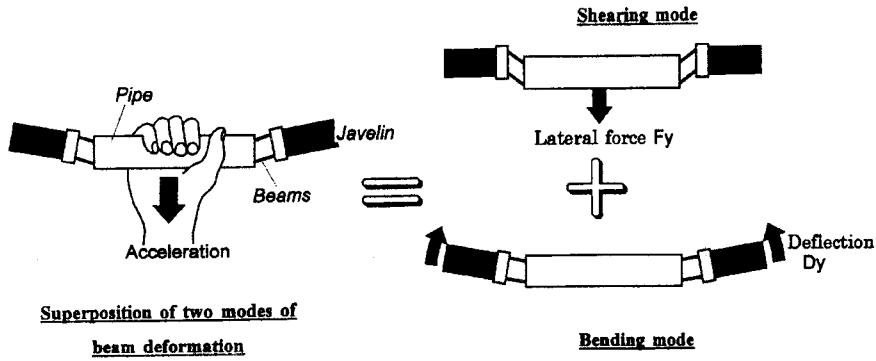

Figure 4 — Example of superposition of force and deflection. Two modes of beam deformation are superposed.

and the changes are canceled in the other seven circuits. In the same way, each Wheatstone bridge circuit is designed to be sensitive to only one corresponding component of force or deflection and to cancel the changes in resistance caused by the other seven components. Furthermore, small crosstalk due to differences in sensitivity of the gauges is compensated by multiplying an 8×8 compensation matrix (discussed below).

Regarding the third difficulty, the pipe, which is supported by the beams and gripped by the thrower, is designed to be thin and light (1 mm in thickness and 0.1092 kg in weight). The present sensor measures the force applied to the beam structure via the gripped pipe F', which is slightly different from the force applied to the grip by

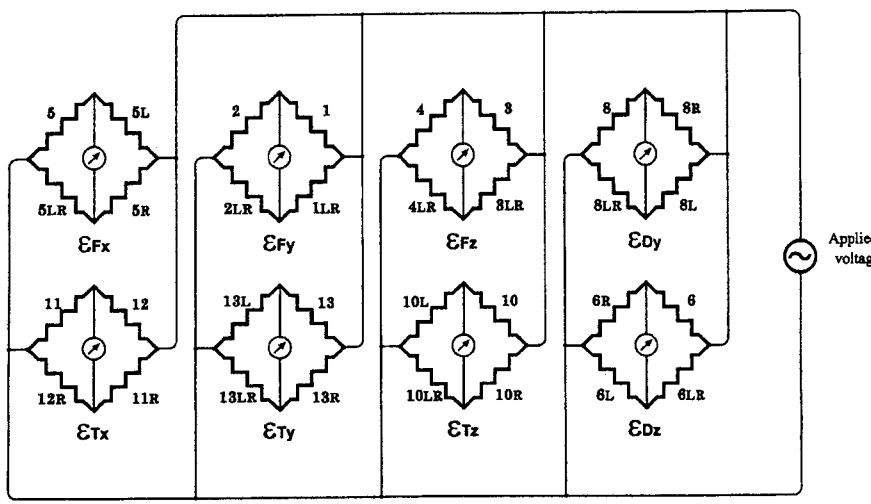

Figure 5 — Construction of Wheatstone bridge circuits. Each circuit is sensitive to only one mode of beam deformation caused by a corresponding component of force or deflection.

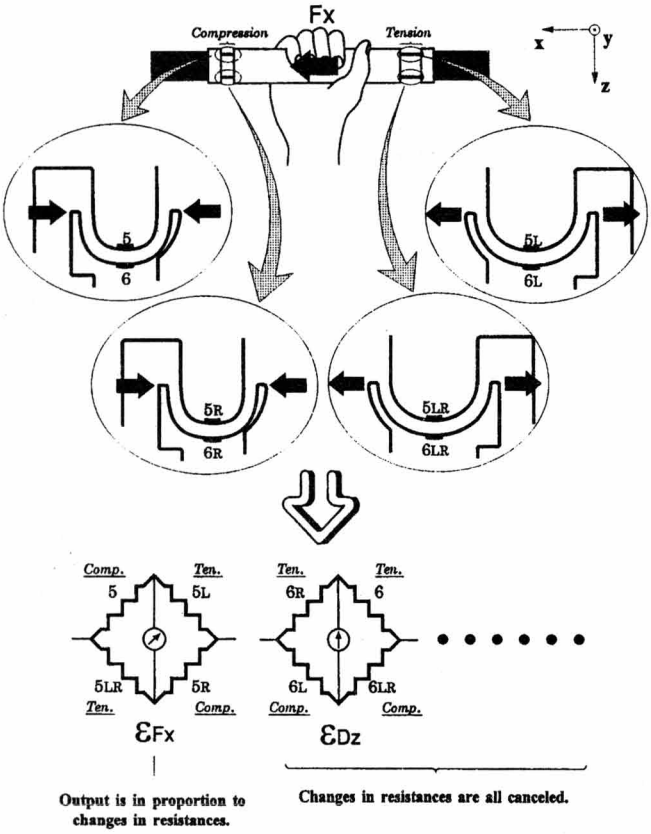

Figure 6 — Schematic illustration of measuring principle. Changes in resistances of gauges in each Wheatstone bridge circuit are added to each other only when one corresponding component of force or deflection is applied.

throwers F when it is accelerated. Below, this small inertial force due to the acceleration of the pipe (i.e., F-F') is estimated and its influence on the measurement is discussed.

Calibration and Characteristics of Developed Sensor

Figure 7a–7d schematically illustrates the setup for calibration of the sensor. The forces and deflections are applied by hanging weights in each direction while the javelin is kept precisely horizontal or vertical with the use of a level. The above mentioned forces F and F' are the same in this calibration, because the forces are applied statically. The deflections Dy' and Dz' are measured as the displacements of the grip center relative to the original straight centerline while the javelin is supported at the two nodal points of the first resonant mode (Figure 7d). Thus, Dy' and Dz' are approximately equal to the deflections Dy and Dz during throwing, since the first resonant mode is considered to be dominant. Note that this is an approximation, because the mode of the static deflection (shown in Figure 7d) is slightly different from the first resonant mode, and the strain

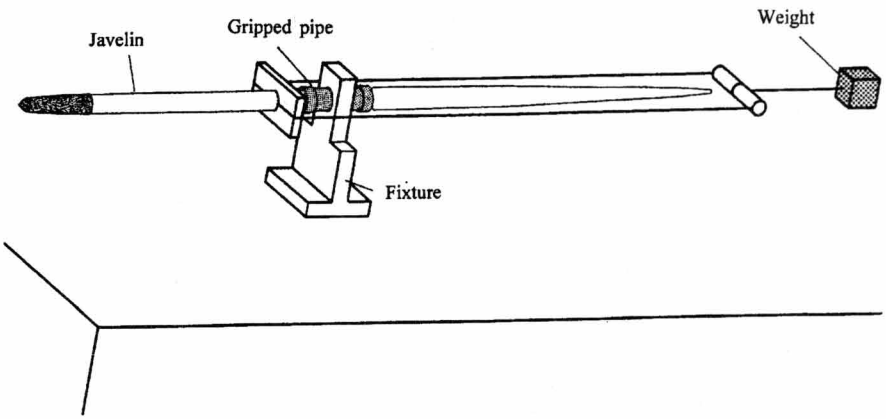

Figure 7a — Calibration of developed sensor for axial force *Fx*. *Fx* is applied by hanging weight, while the gripped pipe is fixed vertically.

gauges measure the curvature of the javelin at the grip ends. According to Euler-Bernoulli beam analysis with an uniform cross section, the actual displacements *Dy* and *Dz* are estimated to be 1.36 times larger than the measured values *Dy'* and *Dz'* if the javelin is deflected in the first resonant mode.

The results of the calibration (i.e., the relationships between the force in each axis and the outputs of all Wheatstone bridge circuits) are shown in Figure 8. *Dy'* and *Dz'*

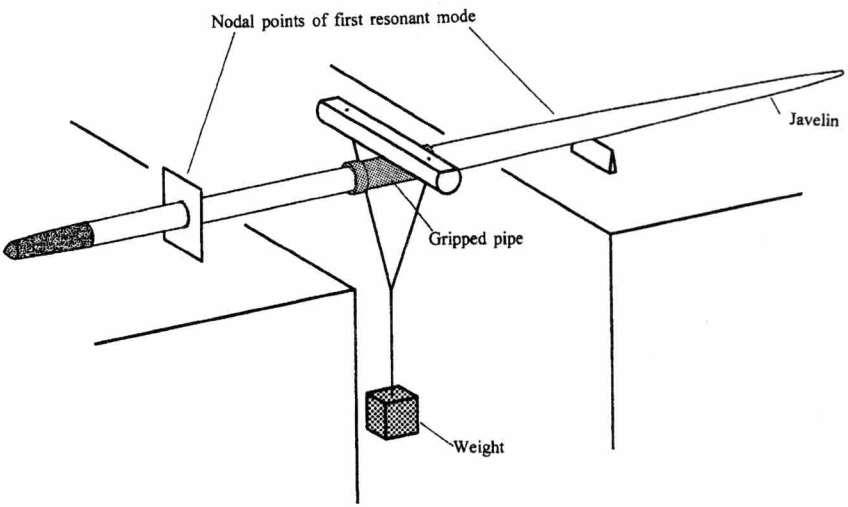

Figure 7b — Calibration of developed sensor for lateral forces *Fy* and *Fz*, and torques *Ty* and *Tz*. *Fy* and *Fz* are applied with deflections *Dy* and *Dz* by hanging weight at the center of the gripped pipe. *Ty* and *Tz* are applied with *Fz* and *Dz*, and *Fy* and *Dy*, respectively, by hanging weight at the end of the pipe. The javelin is supported horizontally at the two nodal points of the first resonant mode.

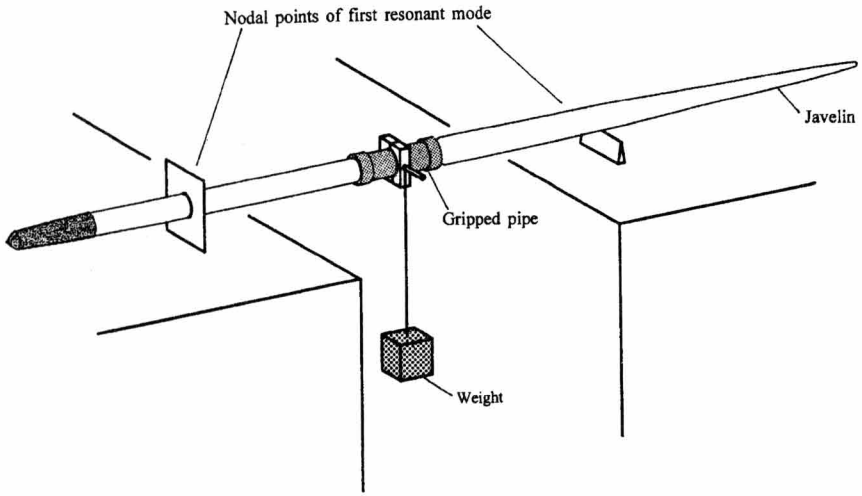

Figure 7c — Calibration of developed sensor for axial torque *Tx*. *Tx* is applied with *Fy* and *Dy* by hanging weight, while the javelin is supported horizontally at the two nodal points of the first resonant mode.

are expressed as forces in this figure that can be converted into the above mentioned displacements by multiplying by the compliance of the javelin 0.074 mm/N. Since *Fy'*, *Fz'*, *Tx'*, *Ty'*, and *Tz'* are difficult to apply individually by weights, the strains due to these forces (shown in Figure 8) are calculated by subtracting the strains due to the other

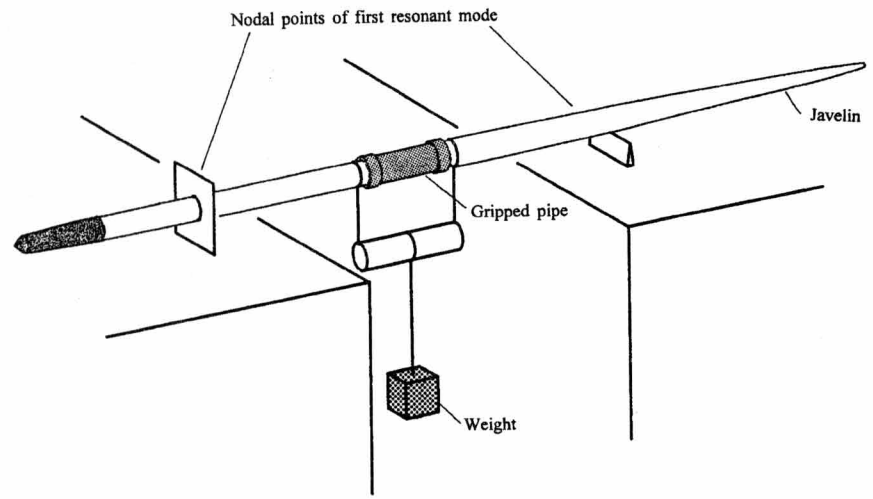

Figure 7d — Calibration of developed sensor for deflections *Dy* and *Dz*. *Dy* and *Dz* are applied by hanging weight, while the javelin is supported horizontally at the two nodal points of the first resonant mode.

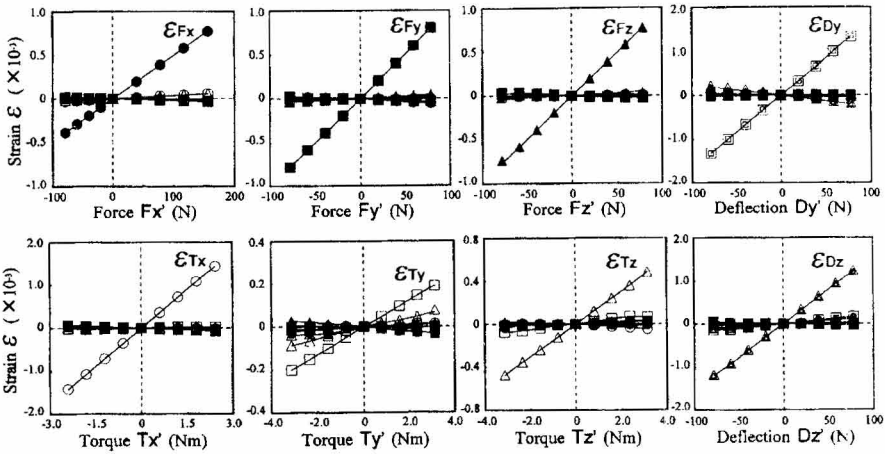

Figure 8 — Force in each axis and outputs of all Wheatstone bridge circuits. Each relationship is measured by changing weights and turning javelin upside down.

forces applied simultaneously. For example, when Fy' is applied as shown in Figure 7b, Dy' is also applied simultaneously. Thus, the strains plotted against Fy' in Figure 8 are calculated by subtracting the strains due to Dy' from those due to Fy' and Dy'. As shown in Figure 8, the developed sensor has good linearity and small crosstalk. The crosstalk is further compensated by utilizing the following compensation matrix (Hatamura, 1986) for precise measurement.

$$\{F'\} = [C]\{\epsilon\}$$

where $\{F'\}$ is the vector of force applied to beam structure via gripped pipe, $[C]$ is the compensation matrix, and $\{\epsilon\}$ is the vector of strain measured by Wheatstone bridge circuits, or

$$\begin{Bmatrix} Fx' \\ Fy' \\ Fz' \\ Tx' \\ Ty' \\ Tz' \\ Dy' \\ Dz' \end{Bmatrix} = \begin{bmatrix} 195.35 & -5.30 & -4.69 & 3.23 & 3.06 & -2.31 & 0.55 & -4.18 \\ 9.91 & 122.01 & 5.11 & 9.79 & -0.88 & 3.29 & 0.78 & 2.12 \\ 7.85 & -10.25 & 122.23 & 8.37 & -8.62 & 5.17 & -1.70 & 1.32 \\ 1.35 & -0.01 & -0.03 & 1.95 & 0.04 & -0.01 & 0.02 & -0.08 \\ -0.02 & 0.42 & 0.14 & -0.08 & 5.54 & 1.08 & 0.06 & -0.04 \\ 0.03 & -0.26 & -0.43 & -0.11 & -0.87 & 6.51 & 0.01 & -0.24 \\ -0.03 & -0.36 & 0.12 & -0.01 & 0.06 & -0.19 & 4.38 & -0.52 \\ 0.04 & 0.09 & -0.02 & 0.08 & -0.12 & -0.09 & 0.52 & 4.19 \end{bmatrix} \begin{Bmatrix} \epsilon_{Fx} \\ \epsilon_{Fy} \\ \epsilon_{Fz} \\ \epsilon_{Tx} \\ \epsilon_{Ty} \\ \epsilon_{Tz} \\ \epsilon_{Dy} \\ \epsilon_{Dz} \end{Bmatrix}$$

where Fx', Fy', Fz', Tx', Ty', and Tz' are the six components of force applied to beam structure; Dy' and Dz' are the two components of deflection of javelin calibrated by static load; and ϵ_{Fx}, ϵ_{Fy}, ϵ_{Fz}, ϵ_{Tx}, ϵ_{Ty}, ϵ_{Tz}, ϵ_{Dy}, and ϵ_{Dz} are outputs of Wheatstone bridge circuits. The units of the first, second, and third columns in the compensation matrix are N; the fourth, fifth, and sixth columns, Nm; and the seventh and eighth columns, mm.

Table 1 Applied Force and Measuring Errors After Utilizing Compensation Matrix

Fx' (N)	Error in Fx' (%)	Fy' (N)	Error in Fy' (%)	Error in Fz' (%)	Tx' (Nm)	Error in Tx' (%)	Ty' (Nm)	Error in Ty' (%)	Error in Tz' (%)	Dy' Dz' (N)	Error in Dy' (%)	Error in Dz' (%)
156.8	0.63	78.4	0.88	-0.61	2.4	1.13	3.1	1.04	-4.49	78.4	1.35	0.13
117.6	0.57	58.8	0.07	-0.99	1.8	0.93	2.4	-1.81	-4.74	58.8	0.66	0.55
78.4	0.08	39.2	0.16	-0.10	1.2	0.66	1.6	-0.70	-4.17	39.2	-0.01	0.07
39.2	1.31	19.6	-3.80	1.85	0.6	0.43	0.8	-3.89	-3.02	19.6	-1.90	0.08
0	0	0	0	0	0	0	0	0	0	0	0	0
-19.6	-1.03	-19.6	3.04	0.27	-0.6	-2.84	-0.8	-0.43	3.71	-19.6	-1.25	-2.02
-39.2	-1.24	-39.2	0.70	-0.15	-1.2	-0.84	-1.6	0.67	3.92	-39.2	-0.45	-0.70
-58.8	-1.77	-58.8	-1.16	-0.02	-1.8	-0.46	-2.4	0.14	3.64	-58.8	0.11	-0.03
-78.4	-1.26	-78.4	-0.47	0.24	-2.4	-0.04	-3.1	-2.77	2.15	-78.4	0.14	0.47

The above compensation matrix $[C]$ is calculated from the relationships between $\{F'\}$ and $\{\epsilon\}$ shown in Figure 8, where the inclinations of the 64 lines (i.e., ϵ_{Fx}/Fx', ϵ_{Fy}/Fx', ϵ_{Fz}/Fx', etc.) are the elements of the inverse compensation matrix $[C]^{-1}$. After compensation, the remaining errors between the applied force and the measured one are small as shown in Table 1. The measuring errors are less than 4% in each component of the force and the deflection.

Figure 9 shows the frequency responses of the sensor, which are measured by employing the impulse response method, where the input is the applied force measured by a commercial piezoelectric force transducer fixed to the impulse hammer, and the output is the force measured and compensated for by the compensation matrix. As

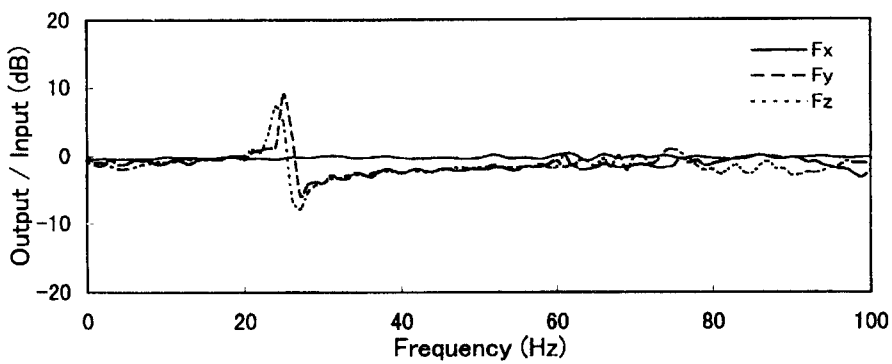

Figure 9 — Frequency responses of developed force sensor in force components Fx', Fy', and Fz'. Input: force measured by commercial force transducer fixed to impulse hammer. Output: force measured and compensated for. Vertical axis: output/input after Fourier transformation of impulse forces to frequency domain.

Table 2 Basic Characteristics of Javelin With Force Sensor and Ordinary Javelin

Variable	Javelin with sensor	Ordinary javelin
Length (m)	2.603	2.615
Mass (kg)	0.8135	0.8108
Center of gravity (m)	1.058	1.056
Grip (m)	1.204	1.206
Moment of inertia (kgm^2)		
Around lateral direction	0.307	0.411
Around axial direction	0.133×10^{-3}	0.128×10^{-3}
Resonant frequency (Hz)	25.6	25.9

Note. Center of gravity is distance from tip to center of gravity; grip is distance from tip to end of grip; and moment of inertia is the moment of inertia around center of gravity.

shown in Figure 9, the response in gain of the sensor (i.e., magnitude of output/input after Fourier transformation of the impulse forces to the frequency domain) is almost constant, within ±0.7 dB in *Fx* in a wide range of frequencies up to 100 Hz. This means that the axial force *Fx* measured by the present sensor is almost the same as that measured by the reliable piezoelectric force transducer over a sufficient range of frequency. *Fy* and *Fz* measured by the present sensor have large errors of about ±8 dB around 25 Hz due to the vibratory deflection at the first resonant vibration. The influence of this dynamic characteristic of the sensor on the practical measurement is discussed below.

The basic characteristics of the javelin (Maeda et al., 1990; Maeda et al., 1993) equipped with the sensor and an ordinary javelin are compared in Table 2. Most of their characteristic values are similar, although the javelin with the sensor has a slightly smaller moment of inertia around the lateral direction compared to the ordinary one.

Measurement of Force and Deflection Applied to Javelin

Measuring System

The experimental setup to measure the force and the deflection applied to the javelin is shown in Figure 10. Six components of the force and two components of the deflection applied to the javelin are measured for a period from run-up to release by using the present measuring system. The throwing motion is videotaped simultaneously on the right side of the throwing area by a high-speed video camera operating at 200 frames per second. A small connector is set up between the sensor and the thrower so that the sensor is disconnected from the strain amplifiers just after the javelin is released. The outputs from the eight Wheatstone bridge circuits are recorded in a computer via A/D converters together with a pulse signal generated at each frame of the high-speed video image. The sampling frequency of the A/D converters is 1 kHz.

Subject

The subject was a male Japanese javelin thrower with a height and weight of 1.83 m and 93.0 kg, respectively. He was considered a middle class thrower, and his best record was 65.68 m.

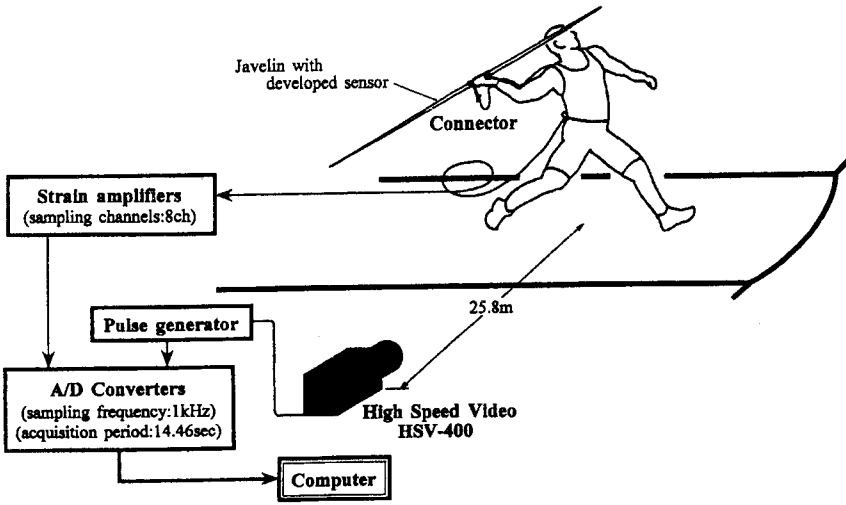

Figure 10 — Experimental setup for measurement during throwing. Force and deflection are recorded by personal computer via strain amplifiers and A/D converters synchronized with high-speed video images.

Measurement of Force and Deflection Applied to Javelin in Throwing

Figure 11 shows an example of the measured force and deflection applied to the javelin in throwing. The pictures labeled from (a) to (g) show the throwing forms at different moments. The horizontal axis is time, and the moment of release of the javelin (see picture (g)) is chosen to be zero. *Fyz′*, *Tyz′*, and *Dyz′* are resultant vectors of *Fy′* and *Fz′*, *Ty′* and *Tz′*, and *Dy′* and *Dz′*, respectively.

The peaks of the force components appear just before the release of the javelin, and the peak forces are 192 N in the axial direction and 233 N in the lateral direction. The peak torques are 1.4 Nm and 7.6 Nm around the axial and lateral directions, respectively. The peak deflection is 18.1 mm.

It has been reported that the main throwing motion starts at the moment (d) when the left foot touches the ground and ends at the moment (g) when the javelin is released. However, it should be noted that the forces start to rise at the moment (c) before the left foot touches the ground.

At the moment (f), all components become almost zero except *Fx*, and the axial force *Fx* decreases slightly. These correspond to the lateral rotation of the shoulder with bending of the elbow as shown in the picture (f).

After release, the force components become almost zero, while the deflection remains oscillatory. This indicates that the javelin is released with the remaining vibratory deflection.

Estimation of Inertial Force Applied to Gripped Part

The present sensor measures the force applied to the beam structure via the gripped pipe *F′*, which is slightly different from the force applied to the grip by the thrower *F* when

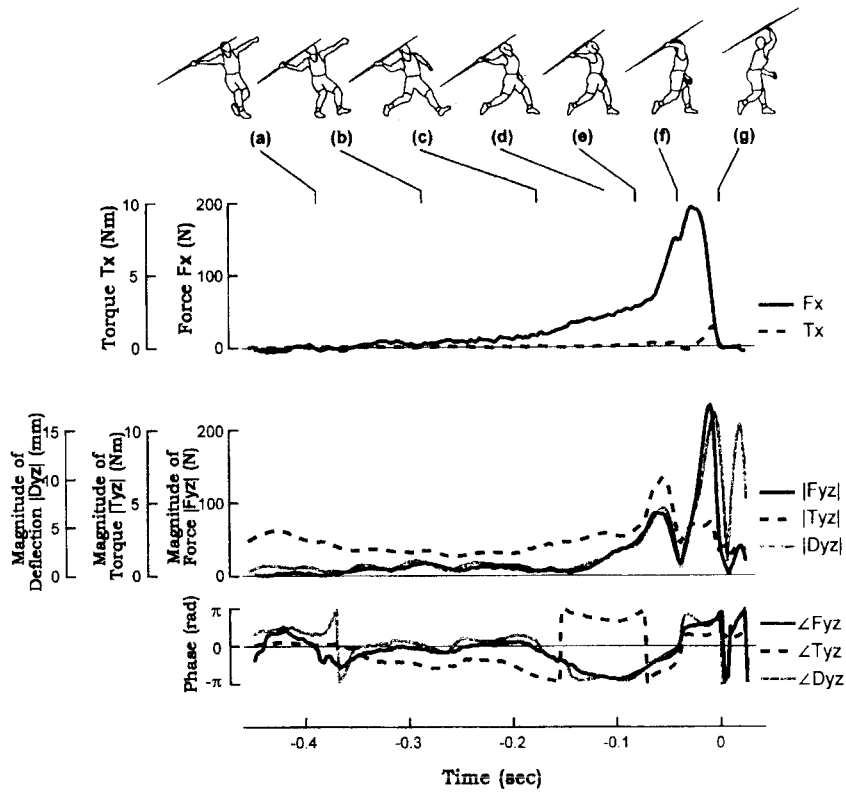

Figure 11 — Components of force and deflection measured during throwing. *Fx'* and *Tx'* are the forces in the axial direction and the torque around the axial direction, respectively. |*Fyz'*|, |*Tyz'*| and |*Dyz'*| are magnitudes of resultant force in the lateral direction, resultant torque around the lateral direction, and the resultant deflection, respectively. *Fyz'*, *Tyz'*, and *Dyz'* are their phases. Pictures (a)–(g) are copied from high-speed video images taken at corresponding moments.

it is accelerated. In order to obtain the small inertial force (i.e., the difference $F - F'$), the acceleration applied to the gripped pipe must be known. Although it is difficult to obtain this acceleration precisely, the amount of the inertial force can be estimated roughly by assuming: (a) the javelin is flexible only in the lateral direction y and z, and is deflected in the first resonant mode; (b) the change in the direction of the x axis is negligible; (c) the deformation of the beams is negligible, and (d) the lateral force Fyz and the deflection Dyz is applied only in one direction while the javelin is rotated.

$\angle Fyz'$ or $\angle Dyz'$ shown in Figure 11 is the relative rotational angle of the javelin to the ground plus the change in the phase angle of the lateral force applied by the thrower. The above assumption is equivalent to assuming that the latter angle is negligible compared to the former. Figure 12 shows the lateral force Fyz' and the deflection Dyz' (assumed to be unidirectional), which are obtained by adding a positive or negative sign to the magnitudes of the vectors. Under the above assumptions, the axial force and torque Fx and Tx, and the lateral torque Tyz are proportional to the measured com-

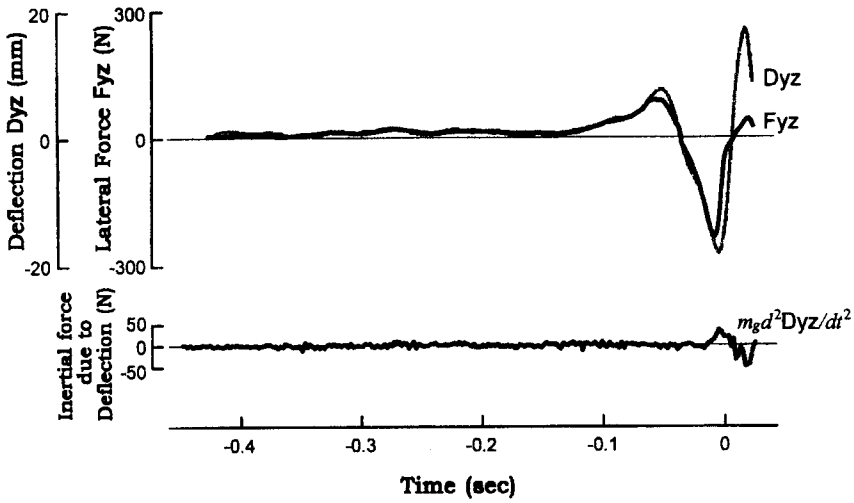

Figure 12 — Lateral force *Fyz'* and deflection *Dyz'* assumed to be unidirectional, and estimated inertial force applied to gripped part due to deflection $m_g d^2Dyz'/dt^2$.

ponents *Fx'*, *Tx'*, and *Tyz'* and are slightly larger than the measured ones, while only the lateral force *Fyz* is affected by the vibratory deflection *Dyz* as follows.

$$Fx \approx Fx' + m_g \frac{d^2x}{dt^2} \approx Fx' + m_g \frac{Fx'}{m_j - m_g} = \frac{m_j}{m_j - m_g} Fx' = 1.16\, Fx'$$

$$Fyz \approx Fyz' + m_g \frac{d^2yz}{dt^2} \approx Fyz' + m_g \left(\frac{Fyz'}{m_j - m_g} + \frac{d^2Dyz'}{dt^2} \right) = 1.16\, Fyz' + m_g \frac{d^2Dyz'}{dt^2}$$

$$Tx \approx Tx' + I_g \frac{d^2\theta x}{dt^2} \approx Tx' + I_g \frac{Tx'}{I_j - I_g} = \frac{I_j}{I_j - I_g} Tx' = 1.02\, Tx'$$

$$Tyz \approx Tyz' + J_g \frac{d^2\theta yz}{dt^2} \approx Tyz'$$

where *Fx*, *Fyz*, *Tx*, and *Tyz* are components of force applied to grip by the thrower; *x* and *yz* are axial and radial positions of gripped part; θx and θyz are rotational angle around axial direction and resultant rotational angle around lateral direction; $m_g = 0.1092$ kg is the mass of gripped part; $m_j = 0.8135$ kg is the mass of javelin including gripped part; $I_g = 0.02 \times 10^{-3}$ kg m^2 is the moment of inertia of gripped part around axial direction; $I_j = 0.133 \times 10^{-3}$ kg m^2 is the moment of inertia of javelin around axial direction; and $J_g = 0.52 \times 10^{-3}$ kg m^2 is the moment of inertia of the gripped part around the lateral direction. The influence of the deflection on the lateral force $m_g d^2Dyz'/dt^2$ is calculated numerically in Figure 12. As shown in the figure, the measurement error due to this influence is negligible for most of the throwing period, although it reaches 15% of the

peak force just before release. The maximum error of 15% becomes 21% when considering the 1.36 ratio calculated by Euler-Bernoulli beam analysis.

In summary, all force components applied to the javelin via the beams $\{F'\}$ including the deflection Dyz' can be measured precisely with the present system, and the axial force and torque Fx and Tx, and the lateral torque Tyz can be obtained using the above equation. Only the lateral force Fyz contains a relatively large error, which is estimated to be a maximum of 21% of the peak force.

Conclusion

A new force sensor was developed to measure six components of the force and two components of the deflection applied to the javelin during the javelin throw. The force sensor and the javelin are designed to cope with the difficulties found in particular in the force measurement of the javelin throw, and it was confirmed that the sensor developed here has good linearity and small crosstalk. Based on this research, it is hoped that the throwing process and the dynamic interaction between the throwers and the javelin will be better understood.

References

Hatamura, Y. (1986). Force and torque sensor. *Journal of the Japan Society of Mechanical Engineers*, **89**, 1055-1058. (in Japanese)

Hubbard, M., & Bergman, C.D. (1989). Effect of vibrations on javelin lift and drag. *International Journal of Sport Biomechanics*, **5**, 40-59.

Maeda, M., Nomura, H., & Miyagaki, M. (1990). Static characteristics of javelin—Form and moment of inertia. *Research Quarterly for Athletics*, **2**, 18-28. (in Japanese)

Maeda, M., Nomura, H., Moriwaki, T., & Shamoto, E. (1993). Dynamic characteristics of javelin. *Japanese Journal of Sports Sciences*, **12**, 130-136. (in Japanese)

Maeda, M., Nomura, H., Shamoto E., & Moriwaki, T. (1994). Measurement of force applied to javelin in javelin throw. *Japan Journal of Physical Education*, **39**, 109-117. (in Japanese)

Terauds, J. (1985). *Biomechanics of the javelin throw*. Del Mar, CA: Academic.